Non-Markovian Exciton-Phonon Interactions in Core-Shell Colloidal Quantum Dots at Femtosecond Timescales

A. Liu,[1] D. B. Almeida,[1] W. K. Bae,[2] L. A. Padilha,[3] and S. T. Cundiff[1,*]
[1]Physics Department, University of Michigan, Ann Arbor, Michigan 48109, USA
[2]SKKU Advanced Institute of Nano Technology, Sungkyunkwan University, Gyeonggi 16419, Republic of Korea
[3]Instituto de Fisica "Gleb Wataghin," Universidade Estadual de Campinas, 13083-970 Campinas, Sao Paulo, Brazil

(Received 22 May 2018; revised manuscript received 21 June 2019; published 2 August 2019)

We perform two-dimensional coherent spectroscopy on CdSe/CdZnS core-shell colloidal quantum dots at cryogenic temperatures. In the two-dimensional spectra, sidebands due to electronic coupling with CdSe lattice LO-phonon modes are observed to have evolutions deviating from the exponential dephasing expected from Markovian spectral diffusion, which is instantaneous and memoryless. Comparison to simulations provides evidence that LO-phonon coupling induces energy-gap fluctuations on the finite timescales of nuclear motion. The femtosecond resolution of our technique probes exciton dynamics directly on the timescales of phonon coupling in nanocrystals.

DOI: 10.1103/PhysRevLett.123.057403

Colloidal quantum dots (CQDs), semiconductor nanocrystals dispersed in solution, are the continued focus of intense study due to their applications in many areas including biological tagging [1], display technologies [2], and photovoltaics [3]. The comprehensive understanding of carrier dynamics required for CQD applications is hindered by complexities resulting from electronic states coupling to external degrees of freedom, such as vibrational modes or charge configurations.

Fluctuations in the exciton resonance energy due to interactions with the local environment, called spectral diffusion, comprise the microscopic origin of dephasing and are not well understood. Though such fluctuations have been mitigated in other nanostructures, such as self-assembled dots [4,5], this is not true for CQDs [6–9]. Spectral diffusion, which may be thought of as dynamic inhomogeneous broadening, is challenging to study via one-dimensional spectroscopic techniques since CQD ensembles possess inherent static inhomogeneous broadening due to dot size dispersion. Elucidating the physical origins of resonance energy fluctuations in CQDs is vital to optoelectronic applications of the material.

The interactions of excitons with their surroundings may be considered either Markovian (resonance energy fluctuations are instantaneous and uncorrelated) or non-Markovian (timescales of the interactions and exciton dynamics are comparable, and energy fluctuations are correlated). In the Markovian regime, coherences dephase exponentially at a rate $1/T_2$ and the physical origins of the dephasing mechanisms are obscured. In the non-Markovian regime however, the physical nature of the dephasing interactions manifests as nonexponential evolution of coherences [10]. Though it is known that phonon coupling in semiconductors may induce non-Markovian dephasing [11], the ns temporal resolution limit of spectrally-resolved single dot studies [12,13] exceeds the correlation time of the vibrational coupling in CQDs [14]. Indeed, without access to exciton dynamics at timescales of the vibrational coupling itself, studies of CQDs and their optical properties have thus far assumed effective homogeneous broadening in the Markovian limit [15–18]. A technique capable of circumventing inhomogeneous broadening with femtosecond time resolution is thus necessary to reveal signatures of non-Markovian dynamics in CQDs.

Multidimensional coherent spectroscopy (MDCS) [19] is a technique able to unfold the optical response of an inhomogeneous ensemble of emitters with femtosecond time resolution by correlating absorption, intraband (Raman) [20], and emission spectra. By simultaneously resolving the response of all constituent frequency groups within the excitation bandwidth, the homogeneous response of inhomogeneously broadened systems may be efficiently studied [21,22]. However, MDCS studies on CQDs are scarce and have been primarily at room temperature [18,23–26], where coherences dephase in the Markovian regime due to the large equilibrium phonon population.

In this Letter, we apply MDCS at cryogenic temperatures to study coherent dynamics of a CdSe CQD ensemble on the femtosecond timescale. Spectrally separating third-order responses that involve intraband coherences from those that involve population states reveals differing temporal behaviors. Comparison to simulation provides further evidence that strong modification of exciton dephasing occurs via coupling to longitudinal-optical (LO) vibrational modes [27–29]. Beyond simply increasing the transition homogeneous linewidth [18,30], we observe, for the first time, that LO-coupling induces non-Markovian dynamics

that directly reflect the resonance energy modulation by nuclear motion in the nanocrystal.

MDCS records a four-wave-mixing (FWM) signal generated by three laser pulses as a function of two interpulse delays (τ and T) and evolution time (t) after the third pulse. The coherences excited by each pulse and their evolution frequencies are spectrally resolved and correlated by Fourier transforming the signal along their respective time axes. Most commonly, the transformed variables are τ and t, which results in a one-quantum spectrum with the conjugate axes to τ and t representing the absorption frequency ω_τ and emission frequency ω_t, respectively. The coherence generated by the first pulse evolves with negative phase for the rephasing signals [31] measured here, which is reflected in negative values of ω_τ. In this study, we also record the signal as a function of delay T and transform with respect to T and t, which generates a zero-quantum spectrum with the same emission frequency axis and the conjugate axis of T representing the intraband coherence mixing frequency [32] ω_T.

We use a multidimensional optical nonlinear spectrometer (MONSTR) [33], which splits 90 fs pulses (collinearly polarized, at a repetition rate of 250 kHz, and centered at a wavelength of 605 nm) into four identical copies that are independently delayed and arranged in the box geometry. An excitation intensity of 4 W/cm^2 generates a predominately third-order response as verified by power dependence of the heterodyned signal. We study CdSe/CdZnS core-shell CQDs of 2 nm core radius and 2.5 nm shell thickness suspended in heptomethylnonane whose synthesis procedure is detailed elsewhere [34]. The sample optical density is 0.3 at the room-temperature 1S exciton absorption peak.

One-quantum spectra were acquired at a temperature of 20 K for delay T increasing from 0 fs to 675 fs at 25 fs intervals. All spectra were relatively phased by maximizing the absorptive line shape for one quadrature. We plot in Figs. 1(a) and 1(b) the one-quantum spectrum at $T = 0$ and a slice perpendicular to the diagonal line. Two prominent features of the spectrum are a zero-phonon line at $\Delta E = E_t - E_\tau = 0$ and a surrounding broad pedestal at $|\Delta E| < 10$ meV due to coupling with lattice acoustic phonon modes, which we will discuss in a future paper. Here, we focus on sidebands observed at energies $\Delta E \approx \pm 26$ meV (matching the LO phonon mode energy $\hbar\omega_{\mathrm{LO}}$ of CdSe [35]), which are highlighted by the green and yellow arrows in Figs. 1(a) and 1(b). In Fig. 1(c) it can be seen that Fourier transforming the evolution along time T of the complex slices at $\Delta E = -26$ meV reveals a clear peak indicative of quantum oscillations in time T corresponding to allowed intraband coherences at the LO-phonon energy. Such oscillations have previously been observed in three-pulse integrated FWM experiments [36,37], but were not spectrally resolved and correlated in their absorption and emission dynamics.

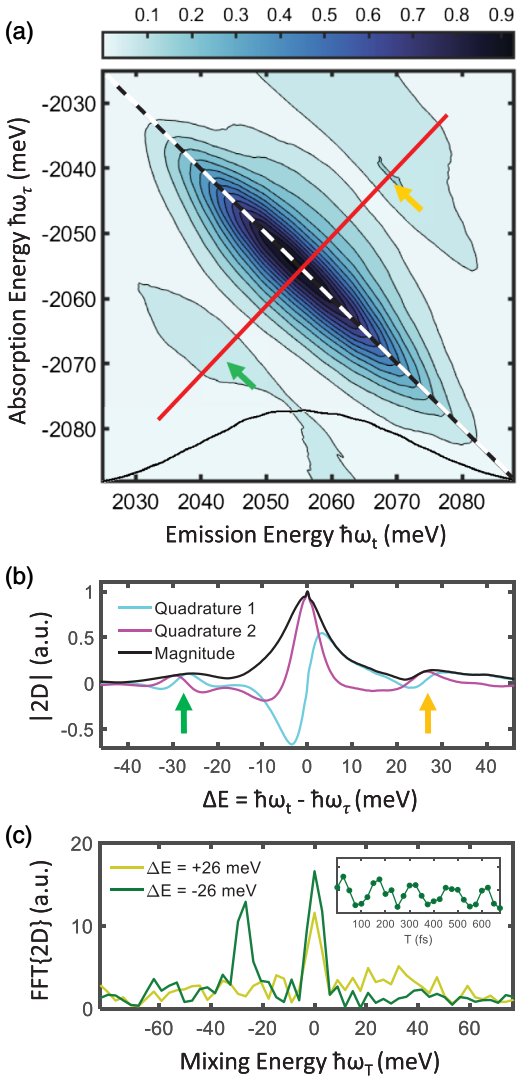

FIG. 1. (a) Magnitude one-quantum spectrum at $T = 0$. The dashed line and solid red line indicate the diagonal ($|\hbar\omega_\tau| = |\hbar\omega_t|$) and plot slice location, respectively. The solid black curve shows the spectrum of the excitation and local oscillator pulses. (b) Magnitude and quadratures of the $T = 0$ plot slice centered at $|\hbar\omega_\tau| = |\hbar\omega_t| = 2055$ meV. (c) Fourier transforms of the (twice zero-padded) complex evolutions of the $\Delta E = -26$ meV and its conjugate $\Delta E = +26$ meV points. These slice positions are marked by arrows in (a) and (b). Inset shows absolute value evolution of the $\Delta E = -26$ meV point.

These one-quantum data reveal two main nonintuitive observations: (1) only the Stokes sideband exhibits oscillations due to the LO-phonon coupling as a function of T and (2) its Fourier spectrum in Fig. 1(c) is one sided. Understanding the origin of these observations will give further insight into the fundamental physical processes in CQDs. Complicating the study of these one-quantum data however, is the fact that the responses involving intraband coherences during T appear at the same coordinates as those involving population states during T. Overlapping pathways on a one-quantum spectrum may be separated by

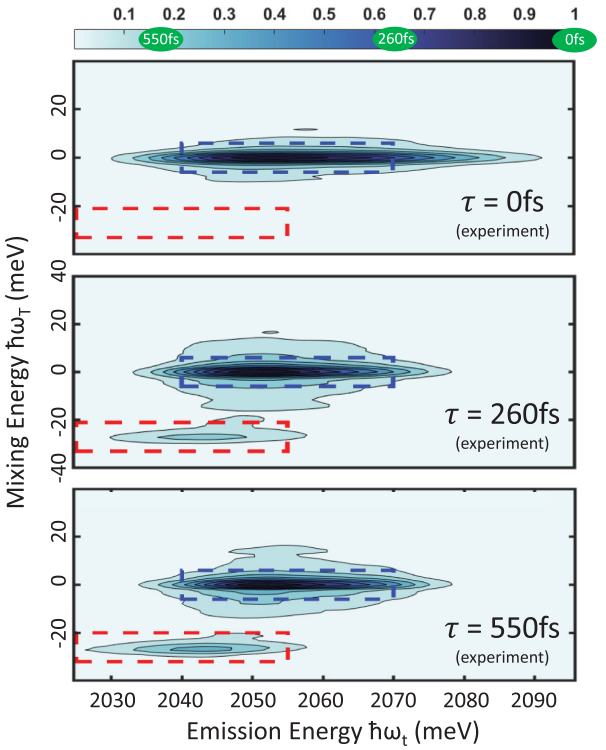

FIG. 2. Zero-quantum plots at $\tau = 0$ fs, 260 fs, and 550 fs as indicated. Dashed blue and red boxes indicate the integrated areas for their respective peak intensities. The relative normalizations of each plot are indicated on the color bar.

spectral filtering of the excitation pulses [38–40]. Another method is to acquire zero-quantum spectra, which spectrally separate intraband coherence pathway responses from population state responses directly [32]. We thus acquire zero-quantum spectra at τ spanning 0 fs to 550 fs, three of which are plotted in Fig. 2. As τ increases, a sideband appears at the LO-phonon energy $\omega_T = -26$ meV. There is also an asymmetry in the sideband formation as no peak is observed at $\omega_T = +26$ meV, agreeing with the one-sided spectrum in Fig. 1(c). Most interestingly, integrating the spectrum over the blue and red dashed rectangles shown in Figs. 2 and 3(b) reveals that both peaks strengthen during early τ (130 fs for the $\omega_T = 0$ peak and 250 fs for the sideband). The full evolutions are shown in Figs. 3(c) and 3(d). To explain these observations, we simulate the system's response and its resultant zero-quantum spectra.

We simulate the optical response in two ways. First, we model the resonant exciton transition coupled to both acoustic continuum phonon and discrete LO-phonon modes (see Supplemental Material [42]). Their spectral densities [10], which characterize the frequency-dependent exciton-phonon coupling strength, are taken to be a Lorentzian centered at the LO-phonon energy [43] and a super-Ohmic acoustic phonon spectral density derived for a spherical quantum dot [44,45] with parameters found by comparison to one-quantum spectra [46]. To gain physical insight, we then neglect coupling to acoustic phonon modes and simulate a system of levels consisting of Franck-Condon transitions between ground and excited state manifolds formed from ladders of states separated by the LO-phonon energy [47]. The oscillator strengths between states are proportional to their respective Franck-Condon factors [48], which are functions of the Huang-Rhys parameter S (characterizing the electronic-vibrational coupling strength) and the initial or final vibrational excitation number m/n. Because of our laser bandwidth of 30 meV and decreasing transition strength with higher m and n, it is assumed that the main transitions contributing to the signal occur between the zeroth and first vibrational states in the ground $\{|g\rangle, |\tilde{g}\rangle\}$ and excited state manifolds $\{|e\rangle, |\tilde{e}\rangle\}$ as shown in Fig. 3(a) The ensemble-averaged transitions between these states then form the peaks of the simulated zero-quantum spectrum in Fig. 3(b). We simplify our simulation in two ways. First, since the sample temperature of 20 K is much lower than the LO-phonon Boltzmann temperature of 302 K, we assume all excited CQDs begin in the ground state $|g\rangle$. Second, we repeated the zero-quantum experiment with co- and cross-circularly polarized excitation and observed the same peak behaviors. Because the CQD selection rules dictate (suppression) enhancement of doubly excited transitions by (co-) cross-circular excitation [49], we neglect transitions into doubly excited states in the simulations.

To relate the observed peaks to evolution of coherences and populations, Feynman diagrams are used, which represent the quantum pathways that compose the system's perturbative response [10]. The signal measured in the phase-matched direction is generated as follows: (1) The first pulse generates an interband coherence that evolves during τ at an energy within the laser spectrum, called a one-quantum coherence. (2) The second pulse generates either a population state or an intraband coherence that evolves during T at an energy within the laser bandwidth, called a zero-quantum coherence. (3) The third pulse generates the last interband (one-quantum) coherence that radiates as a coherent FWM signal during t. Explanations of how the pathways represented by each diagram map onto peaks of a zero-quantum spectrum are given in the Supplemental Material [42] and by Yang *et al.* [32]. We show in Fig. 3(b) three example diagrams and the positions at which their responses will appear on the simulated zero-quantum spectra.

The quantum pathways associate each peak's rise in τ with evolution of interband coherences generated by the first excitation pulse, and inclusion of non-Markovian dynamics allows for a photon echo integration [50] rise to occur. Non-Markovian dephasing line shapes are commonly obtained by applying the cumulant expansion to the spectral diffusion trajectory $\delta\omega_{ij}(t)$ of a coherence ρ_{ij}, where $i, j = \{g, e, \tilde{g}, \tilde{e}\}$, and truncating at second order [10]

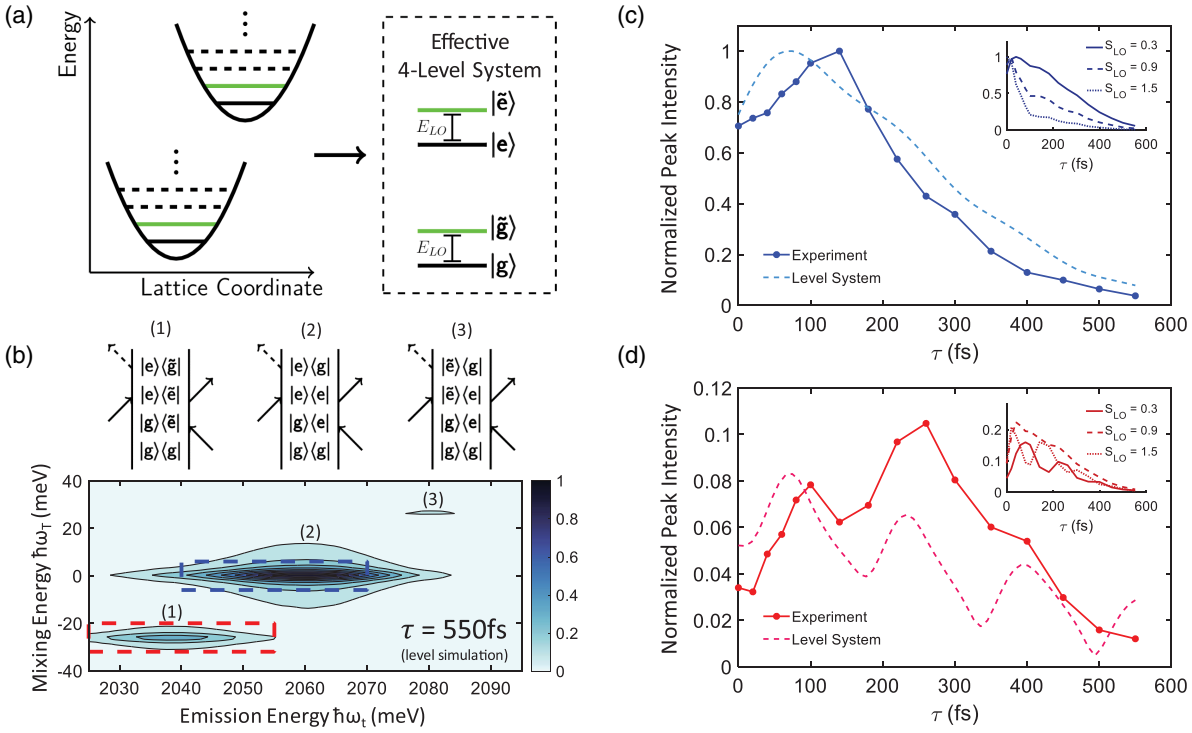

FIG. 3. (a) Schematic of the reduced 4-level system used to interpret the data. (b) Simulated zero-quantum spectrum at $\tau = 550$ fs with the parameters $S = 0.3$, $\tau_c = \tau_c^{\text{vib}} = 1$ ps, $\Delta\omega = 15$ meV, and $\Delta\omega^{\text{vib}} = 3$ meV. Three Feynman diagrams (1), (2), and (3) are shown and their zero-quantum response positions $\{E_{\text{emi}}, E_{\text{mix}}\}$ are $\{E_g - E_{\text{LO}}, -E_{\text{LO}}\}$, $\{E_g, 0\}$, and $\{E_g + E_{\text{LO}}, +E_{\text{LO}}\}$ respectively. (c),(d) Evolution of the experimental and level system simulation $E_{\text{mix}} = 0$ and $E_{\text{mix}} = -E_{\text{LO}}$ peak intensities (integrated over the colored boxed areas in (b)), respectively, as a function of delay τ. The peak intensity evolutions for spectral density simulations that include acoustic mode coupling are plotted inset for $S_{\text{LO}} = 0.3$, 0.9, and 1.5. Oscillations at ω_{LO} in (d) are due to polarization interference [41] between separate quantum pathways.

$$\rho_{ij}(t) \propto e^{-i\omega_{ij}t}\langle e^{-i\int_0^t \delta\omega_{ij}(\tau)d\tau}\rangle \approx e^{-i\omega_{ij}t}e^{-g(t)}, \qquad (1)$$

where the line shape function $g(t)$ is determined by the correlation function $C(t) = \langle\delta\omega_{ij}(t)\delta\omega_{ij}(0)\rangle$ [10]. Though the correlation function may be studied by 3-pulse photon echo peak-shift (3 PEPS) [51,52], reported 3 PEPS data [14,53] are mainly dominated by a fast decrease in peak shift and suffer from ambiguities due to coherent signals during pulse overlap.

A zero-quantum spectrum simulated for the 4-level system in Fig. 3(a) is plotted in Fig. 3(b), with non-Markovian dephasing line shapes from the Kubo ansatz $C(t) = \Delta\omega^2 e^{-(|t|/\tau_c)}$ (where $\Delta\omega$ and τ_c are the amplitude and correlation time of the spectral diffusion) [31]. Comparison between experimental and simulated spectra at $\tau = 550$ fs shows good agreement between peak positions and intensities. Crucially, we achieve this agreement by assigning a large spectral diffusion amplitude $\Delta\omega = 15$ meV to "vibrationless coherences" (ρ_{eg} and ρ_{ge}) and a comparatively smaller amplitude $\Delta\omega^{\text{vib}} = 3$ meV to "coupled coherences" (all ρ_{ij} involving states $\tilde{g}$ and $\tilde{e}$). Because no sidebands appear if $\Delta\omega = \Delta\omega^{\text{vib}}$, the sideband observed in experiment indicates strong modification of dephasing dynamics via coupling to lattice LO vibrational modes. However, Fig. 3(d) shows that matching the decay rate at large τ in both models result in sideband rise times much shorter than the 250 fs rise time observed from experiment. Recently, Gellen *et al.* have reported broadening of the homogeneous linewidth in CQDs due to LO-phonon coupling [18]. However, the discrepancy between experiment and simulation for the zero-quantum sideband evolution indicates that dynamics induced by coupling to LO modes are more complex than simply an increase in the pure-dephasing rate. The non-Markovian signatures observed may indicate an anharmonic phonon bath or even breakdown of the usual second-order cumulant truncation [54]. We emphasize that single-dot studies, which have found similar line shapes for the zero-phonon line and phonon replicas [55], are only sensitive to spectral diffusion at $>$ ns timescales that broaden all features uniformly.

To date, two regimes of spectral diffusion have been identified, on the seconds [56] and sub-μs timescales [12]. Previous studies have focused on free surface charges [13,57] and surface ligand rearrangement [13,56] as possible causes for the band-edge Stark shift [58] that leads to spectral diffusion (to be contrasted with spectral diffusion due to continuum scattering in higher-dimensional systems [59]). The above theories are not sufficient to explain our

results, which clearly point to LO-phonon coupling as a major factor in spectral diffusion on femtosecond timescales. We propose the random environmental perturbations that cause energy gap fluctuations become less dominant when nuclear motion is initiated in the LO mode. The local fields induced by nuclear motion extend over many unit cells—effectively over the entire core volume of our CQDs. For CQDs grown with a shell structure, such as for our sample, it is reasonable to expect that surface charge dynamics are weak compared to Fröhlich coupling between the exciton and local fields that synchronizes the exciton motion with that of the CQD core lattice. The spectral diffusion dynamics then approach timescales on the order of the LO phonon period $T_{\mathrm{LO}} \approx 150$ fs, and non-Markovian evolution of coupled coherences may then occur. It was also found for 3 nm radius bare core (no shell) CQDs the anomalous dephasing dynamics largely disappear (see Supplemental Material [42]). This supports our model, since LO phonon coupling strength has been shown both experimentally and theoretically to vary weakly with dot size in the few-nm size regime [60]. We reason that removal of screening by a shell layer allows surface charge effects to take precedence over LO-phonon coupling.

In conclusion, we have found that spectral diffusion of exciton resonances in CdSe CQDs is strongly modified in the presence of coupled vibrational excitations. The non-Markovian dephasing line shapes we have observed serve as a direct probe of exciton-phonon coupling in CQDs on their intrinsic timescales. In addition to advancing the fundamental understanding of CQDs necessary to mitigate spectral diffusion, these results will prove crucial in applications of systems with strong vibrational coupling towards areas in which pure decoherence is relevant (e.g., single-photon emission [61,62] and quantum information [63,64]) and emphasize the largely unexplored physics of CQDs in the femtosecond temporal regime.

This work was supported by the Department of Energy Grant No. DE-SC0015782. D. B. A. acknowledges support by a fellowship from the Brazilian National Council for Scientific and Technological Development (CNPq). L. A. P. acknowledges support from FAPESP (Projects No. 2013/16911-2 and No. 2016/50011-7).

*cundiff@umich.edu

[1] I. L. Medintz, H. T. Uyeda, E. R. Goldman, and H. Mattoussi, Nat. Mater. **4**, 435 (2005).
[2] J. Eunjoo, J. Shinae, J. Hyosook, L. Jungeun, K. Byungki, and K. Younghwan, Adv. Mater. **22**, 3076 (2010).
[3] X. Lan, S. Masala, and E. H. Sargent, Nat. Mater. **13**, 233 (2014).
[4] H. D. Robinson and B. B. Goldberg, Phys. Rev. B **61**, R5086 (2000).
[5] D. Birkedal, K. Leosson, and J. M. Hvam, Phys. Rev. Lett. **87**, 227401 (2001).
[6] A. A. Cordones and S. R. Leone, Chem. Soc. Rev. **42**, 3209 (2013).
[7] Z. Zhu and R. A. Marcus, Phys. Chem. Chem. Phys. **16**, 25694 (2014).
[8] M. J. Fernee, P. Tamarat, and B. Lounis, Chem. Soc. Rev. **43**, 1311 (2014).
[9] M. I. Lifshitz, L. Z. Tan, J. Tilchin, F. T. Rabouw, M. I. Bodnarchuk, R. J. A. van Dijk-Moes, R. Carmi, Y. Barak, A. Kostadinov, I. Meir *et al.*, J. Phys. B **50**, 214001 (2017).
[10] S. Mukamel, *Principles of Nonlinear Optical Spectroscopy*, 1st ed. (Oxford University Press, Oxford, 1999).
[11] W. A. Hügel, M. F. Heinrich, M. Wegener, Q. T. Vu, L. Bányai, and H. Haug, Phys. Rev. Lett. **83**, 3313 (1999).
[12] L. Coolen, X. Brokmann, P. Spinicelli, and J.-P. Hermier, Phys. Rev. Lett. **100**, 027403 (2008).
[13] A. P. Beyler, L. F. Marshall, J. Cui, X. Brokmann, and M. G. Bawendi, Phys. Rev. Lett. **111**, 177401 (2013).
[14] M. R. Salvador, M. W. Graham, and G. D. Scholes, J. Chem. Phys. **125**, 184709 (2006).
[15] L. Biadala, Y. Louyer, P. Tamarat, and B. Lounis, Phys. Rev. Lett. **103**, 037404 (2009).
[16] F. Masia, N. Accanto, W. Langbein, and P. Borri, Phys. Rev. Lett. **108**, 087401 (2012).
[17] N. Accanto, F. Masia, I. Moreels, Z. Hens, W. Langbein, and P. Borri, ACS Nano **6**, 5227 (2012).
[18] T. A. Gellen, J. Lem, and D. B. Turner, Nano Lett. **17**, 2809 (2017).
[19] S. T. Cundiff and S. Mukamel, Phys. Today **66**, No. 7, 44 (2013).
[20] K. B. Ferrio and D. G. Steel, Phys. Rev. Lett. **80**, 786 (1998).
[21] T. Suzuki, R. Singh, M. Bayer, A. Ludwig, A. D. Wieck, and S. T. Cundiff, Phys. Rev. Lett. **117**, 157402 (2016).
[22] B. Lomsadze and S. T. Cundiff, Science **357**, 1389 (2017).
[23] D. B. Turner, Y. Hassan, and G. D. Scholes, Nano Lett. **12**, 880 (2012).
[24] J. R. Caram, H. Zheng, P. D. Dahlberg, B. S. Rolczynski, G. B. Griffin, A. F. Fidler, D. S. Dolzhnikov, D. V. Talapin, and G. S. Engel, J. Phys. Chem. Lett. **5**, 196 (2014).
[25] C. Y. Wong and G. D. Scholes, J. Phys. Chem. A **115**, 3797 (2011).
[26] S. B. Block, L. A. Yurs, A. V. Pakoulev, R. S. Selinsky, S. Jin, and J. C. Wright, J. Phys. Chem. Lett. **3**, 2707 (2012).
[27] M. Nirmal, C. B. Murray, and M. G. Bawendi, Phys. Rev. B **50**, 2293 (1994).
[28] G. Scamarcio, V. Spagnolo, G. Ventruti, M. Lugará, and G. C. Righini, Phys. Rev. B **53**, R10489 (1996).
[29] D. M. Sagar, R. R. Cooney, S. L. Sewall, E. A. Dias, M. M. Barsan, I. S. Butler, and P. Kambhampati, Phys. Rev. B **77**, 235321 (2008).
[30] P. Palinginis, S. Tavenner, M. Lonergan, and H. Wang, Phys. Rev. B **67**, 201307(R) (2003).
[31] P. Hamm and M. Zanni, *Concepts and Methods of 2D Infrared Spectroscopy*, 1st ed. (Cambridge University Press, Cambridge, England, 2011).
[32] L. Yang, T. Zhang, A. D. Bristow, S. T. Cundiff, and S. Mukamel, J. Chem. Phys. **129**, 234711 (2008).

[33] A. D. Bristow, D. Karaiskaj, X. Dai, T. Zhang, C. Carlsson, K. R. Hagen, R. Jimenez, and S. T. Cundiff, Rev. Sci. Instrum. **80**, 073108 (2009).
[34] L. Jaehoon, J. B. Guk, P. Myeongjin, K. J. Kyeong, J. M. Pietryga, Y.-S. Park, V. I. Klimov, C. Lee, D. C. Lee, and W. K. Bae, Adv. Mater. **26**, 8034 (2014).
[35] M. J. Fernee, C. Sinito, P. Mulvaney, P. Tamarat, and B. Lounis, Phys. Chem. Chem. Phys. **16**, 16957 (2014).
[36] D. M. Mittleman, R. W. Schoenlein, J. J. Shiang, V. L. Colvin, A. P. Alivisatos, and C. V. Shank, Phys. Rev. B **49**, 14435 (1994).
[37] B. Patton, W. Langbein, U. Woggon, L. Maingault, and H. Mariette, Phys. Rev. B **73**, 235354 (2006).
[38] J. O. Tollerud, C. R. Hall, and J. A. Davis, Opt. Express **22**, 6719 (2014).
[39] P. Wen and K. A. Nelson, J. Phys. Chem. A **117**, 6380 (2013).
[40] S. S. Senlik, V. R. Policht, and J. P. Ogilvie, J. Phys. Chem. Lett. **6**, 2413 (2015).
[41] T. Meier, P. Thomas, and S. Koch, *Coherent Semiconductor Optics: From Basic Concepts to Nanostructure Applications*, 1st ed. (Springer, Heidelberg, 2006).
[42] See Supplemental Material at http://link.aps.org/supplemental/10.1103/PhysRevLett.123.057403 for details of the experiment and simulation as well as supplemental data.
[43] J. Seibt and T. Pullerits, J. Phys. Chem. C **117**, 18728 (2013).
[44] T. Calarco, A. Datta, P. Fedichev, E. Pazy, and P. Zoller, Phys. Rev. A **68**, 012310 (2003).
[45] S. Lüker, T. Kuhn, and D. E. Reiter, Phys. Rev. B **96**, 245306 (2017).
[46] A. Liu, D. B. Almeida, W.-K. Bae, L. A. Padilha, and S. T. Cundiff, arXiv:1907.09889.
[47] V. May and O. Kuhn, *Charge and Energy Transfer Dynamics in Molecular Systems*, 3rd ed. (Wiley-VCH Verlag, Weinheim, 2011).
[48] M. de Jong, L. Seijo, A. Meijerink, and F. T. Rabouw, Phys. Chem. Chem. Phys. **17**, 16959 (2015).
[49] G. D. Scholes, J. Chem. Phys. **121**, 10104 (2004).
[50] V. O. Lorenz and S. T. Cundiff, Phys. Rev. Lett. **95**, 163601 (2005).
[51] G. R. Fleming, S. A. Passino, and Y. Nagasawa, Phil. Trans. R. Soc. A **356**, 389 (1998).
[52] V. O. Lorenz, S. Mukamel, W. Zhuang, and S. T. Cundiff, Phys. Rev. Lett. **100**, 013603 (2008).
[53] L. J. McKimmie, C. N. Lincoln, J. Jasieniak, and T. A. Smith, J. Phys. Chem. C **114**, 82 (2010).
[54] H.-B. Chen, N. Lambert, Y.-C. Cheng, Y.-N. Chen, and F. Nori, Sci. Rep. **5**, 12753 (2015).
[55] M. J. Fernee, B. N. Littleton, S. Cooper, H. Rubinsztein-Dunlop, D. E. Gomez, and P. Mulvaney, J. Phys. Chem. C **112**, 1878 (2008).
[56] M. J. Fernée, T. Plakhotnik, Y. Louyer, B. N. Littleton, C. Potzner, P. Tamarat, P. Mulvaney, and B. Lounis, J. Phys. Chem. Lett. **3**, 1716 (2012).
[57] J. Müller, J. M. Lupton, A. L. Rogach, J. Feldmann, D. V. Talapin, and H. Weller, Phys. Rev. Lett. **93**, 167402 (2004).
[58] S. A. Empedocles and M. G. Bawendi, Science **278**, 2114 (1997).
[59] Z. Wang, K. Reimann, M. Woerner, T. Elsaesser, D. Hofstetter, J. Hwang, W. J. Schaff, and L. F. Eastman, Phys. Rev. Lett. **94**, 037403 (2005).
[60] C. Lin, K. Gong, D. F. Kelley, and A. M. Kelley, J. Phys. Chem. C **119**, 7491 (2015).
[61] X. Lin, X. Dai, C. Pu, Y. Deng, Y. Niu, L. Tong, W. Fang, Y. Jin, and X. Peng, Nat. Commun. **8**, 1132 (2017).
[62] V. Chandrasekaran, M. D. Tessier, D. Dupont, P. Geiregat, Z. Hens, and E. Brainis, Nano Lett. **17**, 6104 (2017).
[63] C. E. Pryor and M. E. Flatté, Appl. Phys. Lett. **88**, 233108 (2006).
[64] H.-A. Engel, P. Recher, and D. Loss, Solid State Commun. **119**, 229 (2001).